


**Chaos generated in a semiconductor microcavity**Yong Hong Ma,<sup>\*</sup> Xing Wang Hou, Rong Zhao, and Ming Xin Li*School of Science, Inner Mongolia University of Science and Technology, Baotou 014010, People's Republic of China*Xin Yu Zhao<sup>†</sup>*Department of Physics, Fuzhou University, Fuzhou 350116, People's Republic of China* (Received 8 July 2022; revised 22 October 2022; accepted 17 January 2023; published 28 February 2023)

The dynamics of chaos in quantum systems has attracted much interest in connection with the fundamental aspects of quantum mechanics. We study the chaotic dynamics of both the excitonic mode and the cavity mode in a microcavity containing a quantum well driven by an external field. We investigate how the chaotic dynamics is influenced by the frequencies of the exciton and the cavity, the coupling constant between the exciton and cavity, the Coulomb interaction between excitons, and the response of the exciton to the cavity and the external field. We show that chaos can be generated synchronously in both the cavity and the excitonic mode by choosing appropriate parameters. Moreover, this kind of chaos can be controlled by the coupling constant, the strength of the interaction between excitons, the external field, the response of the excitons to the cavity, and the detuning between the cavity field and the excitonic field. The present study may have applications in chaos-based neural networks and extreme event statistics.

DOI: [10.1103/PhysRevE.107.024220](https://doi.org/10.1103/PhysRevE.107.024220)**I. INTRODUCTION**

The quantum properties of light interacting with a nonlinear medium are a basic research area of modern quantum optics and many-body physics. Chaos, as a nonlinear phenomenon, has been extensively researched in neural networks [1], extreme event statistics [2,3], and biophysics of chaos self-organization [4]. The investigation of chaos and the associated nonlinear dynamics has promoted the development of science and technology [5]. It has been verified that chaos can be used as a powerful tool to suppress decoherence [6,7]. Quantum chaos is also a very important technique to guarantee the high bandwidths communicating masked information [8,9] and high-speed long-distance communication [10]. Moreover, good quality random bit sequences can be generated at very fast bit rates using physical chaos [11–13].

Generally, nonlinear dynamics originates from the coupling between the optical and mechanical modes and thus can lead to the system evolving from periodic to chaotic oscillations. Recently, cavity optomechanics has gained widespread usage in studying quantum optical and nonlinear optical phenomena [14–22]. Beyond cavity optomechanics physics, due to the strongly nonlinear interaction between the exciton and the cavity in semiconductor microcavities, the semiconductor microcavity system has drawn the attention of several theoretical and experimental researchers [23–35], for example, given their potential application in the dynamical behavior of Rabi splitting [27], quantum correlations [28,35–41], the squeezed state of light [42–46], entanglement [47,48], electromag-

netically induced transparency[49], the Autler-Townes effect [50,51], and Coulomb-assisted terahertz transitions [52].

It is well known that a strong driving field can induce period doubling and chaotic dynamics. Due to the similar formulations of the cavity-exciton system and the cavity-oscillator system, a strongly nonlinear interaction between the exciton and the cavity in semiconductor microcavities can also exist. Thus, it can be argued that a semiconductor microcavity should also give rise to period doubling and chaos. However, only Eleuch and Prasad have considered the nonlinear dynamical behavior of the cavity field for a microcavity semiconductor containing a quantum well [53], which in special circumstances allows, for example, weak excitation so that the collective response of the many-exciton system to the cavity [the term  $f(\hat{b}^\dagger \hat{b}^\dagger \hat{b} \hat{a} + \hat{a}^\dagger \hat{b}^\dagger \hat{b} \hat{b})$  in Eq. (1)] is omitted. In this paper we will show that this ignored term is essential in the chaotic phenomenon considered here. They also consider only chaos of the cavity field rather than chaos of phonons in a microcavity semiconductor containing a quantum well. Different from previous studies, we consider a more comprehensive formula where the collective response of the many-exciton system to the cavity is investigated. Moreover, we thoroughly study chaotic dynamics not only for the cavity but also for excitons. This scheme is achieved using a microcavity containing a quantum well driven by an external field. The exciton-cavity system is made to behave as two intrinsic parts, and the behaviors of the chaotic dynamics of the two subsystems are studied. The present research shows that the exciton and the cavity field are simultaneously chaotic by taking appropriate system parameters. We find that the strength of the chaos can be tuned by adjustable parameters  $f$ ,  $g$ ,  $\epsilon$ ,  $\xi$ , and  $\Delta$ . According to the present experiments, the feasible experimental parameters are analyzed.

<sup>\*</sup>Corresponding author: myh\_dlut@126.com<sup>†</sup>Corresponding author: xzhao1@foxmail.com

## II. EFFECTIVE HAMILTONIAN

A microcavity containing a two-band semiconductor embedded between two highly reflecting Bragg mirrors is investigated. The semiconductor is excited optically by the microcavity, resulting in the appearance of many conduction electrons which leave behind holes in the valence band. The distance between the mirrors is of the order of the wavelength. An electron can be excited by the electromagnetic field from the valence band to the conduction band by creating a hole in the valence band. The electron-hole system possesses bound states and excitonic states. As the state  $1s$  is the lowest state which has the greatest oscillator strength, we only consider this state for the exciton-photon interaction. The effective Hamiltonian of the coupled exciton-photon system is given by [43,54]

$$H = \omega_{ph}\hat{a}^\dagger\hat{a} + \omega_{ex}\hat{b}^\dagger\hat{b} + ig(\hat{a}^\dagger\hat{b} - \hat{a}\hat{b}^\dagger) + \xi\hat{b}^\dagger\hat{b}^\dagger\hat{b}\hat{b} + f(\hat{b}^\dagger\hat{b}^\dagger\hat{b}\hat{a} + \hat{a}^\dagger\hat{b}^\dagger\hat{b}\hat{b}) + i\epsilon(\hat{a}^\dagger e^{-i\omega t} - \hat{a}e^{i\omega t}), \quad (1)$$

where  $\hat{a}$  ( $\hat{a}^\dagger$ ) and  $\hat{b}$  ( $\hat{b}^\dagger$ ) represent the annihilation (creation) operators of the cavity field and the exciton, respectively. The first two terms of Eq. (1) are the proper energies of the cavity field and the excitonic field with the frequencies  $\omega_{ph}$  and  $\omega_{ex}$ , respectively. The third term describes the coupling between the exciton and the cavity with the coupling constant  $g$  ( $g$  is a real). The fourth term is the nonlinearity due to the Coulomb interaction between excitons, in which the coefficient  $\xi$  describes the strength of the interaction between excitons. The fifth term means a kind of collective response of the many-exciton system to the cavity: A photon can be absorbed (emitted) to generate (by destroying) an exciton with the assistance of another exciton coexisting in the medium with the former [43]. This kind of process allows excitons with many angular momentum combinations to interact with light [43]. The coefficient satisfies  $f = \frac{16\pi g\lambda_x^2}{7}$ , with  $\lambda_x$  the radius of Bohr of the bidimensional exciton. The last term is the pump term of the laser field, with  $\epsilon$  and  $\omega$  the amplitude and the frequency of the pumping laser, respectively. Note that the fourth and fifth terms in the Hamiltonian (1) can yield coherent nonlinear interaction between the specific mode of interest and the pump mode directly excited by the outside field [55]. Moreover, the damping Hamiltonian is

$$H_{\text{dam}} = \gamma_1\hat{a}^\dagger + \gamma_1^\dagger\hat{a} + \gamma_2\hat{b}^\dagger + \gamma_2^\dagger\hat{b}, \quad (2)$$

where  $\gamma_1$  and  $\gamma_2$  are the decay rates of the cavity field and the exciton, respectively. By solving the Heisenberg equations of motion, stochastic differential equations are employed in the positive- $P$  representation. Based on the conditions of zero temperature and the Born approximation, the equations of the  $c$ -numbers  $\alpha$  ( $\alpha^+$ ) and  $\beta$  ( $\beta^+$ ) can be obtained:

$$\begin{aligned} \dot{\alpha} &= -(\gamma_1 + i\omega_{ph})\alpha + g\beta - if|\beta|^2\beta + \epsilon \exp(-i\omega t), \\ \dot{\alpha}^+ &= -(\gamma_1 - i\omega_{ph})\alpha^+ + g\beta^+ + if|\beta|^2\beta^+ + \epsilon \exp(i\omega t), \\ \dot{\beta} &= -(\gamma_2 + i\omega_{ex})\beta + g\alpha - 2i\chi|\beta|^2\beta \\ &\quad - 2if|\beta|^2\alpha - if\beta^2\alpha^+, \\ \dot{\beta}^+ &= -(\gamma_2 - i\omega_{ex})\beta^+ + g\alpha^+ + 2i\chi|\beta|^2\beta^+ \\ &\quad + 2if|\beta|^2\alpha^+ + if\beta^2\alpha. \end{aligned} \quad (3)$$

These equations allow us to further numerically simulate our analysis of the system. Note that the relationship between the annihilation operators and the quadrature operators is  $\hat{b}(a) = \hat{X}_1(2) + i\hat{P}_1(2)$ , corresponding to the  $c$ -number cases  $\beta(\alpha) = X_1(2) + iP_1(2)$ , that is,  $\text{Re}(\beta)(\alpha) = X_1(2)$  and  $\text{Im}(\beta)(\alpha) = P_1(2)$ .

## III. QUANTUM CHAOS

In this section it will be proved that this system can simultaneously produce two chaotic motions for both the excitonic mode and the cavity mode. We numerically simulate the evolution of the excitonic mode and the cavity mode from two cases in the phase space and frequency domain in Figs. 1 and 2. As shown from Figs. 1(a) and 2(a), the evolutions of the exciton and cavity field are both aperiodic, corresponding to chaotic motion. To get a better view of the chaotic dynamics, the ladder evolution of  $\log_{10} S(\omega)$  is clearly shown in Figs. 1(b) and 2(b). The oblique evolution in the frequency domain signifies exponentially fast separation of neighboring trajectories and that the dynamic evolution of the system is chaotic [21]. The strange attractors can be seen in the phase space in Figs. 1(c) and 2(c). This means that the initial adjacent trajectories eventually become unpredictable diverse states [19,56]. To elucidate the structure of the phase space, we plot the surface of section in Figs. 1(d) and 2(d), which records the quadratures  $\text{Re}(\beta)(\alpha)$  and  $\text{Im}(\beta)(\alpha)$  each time the excitonic (cavity) mode impinges on the cavity boundary, where the unstable periodic orbits are visible.

Another excellent tool for detecting deterministic chaos is characterized by the maximal Lyapunov exponent (LE), which is the signature of the sensitivity of a system to the initial conditions and can measure the divergence of nearby trajectories in phase space [7]. A negative LE shows that the trajectories tend to a common fixed point, while a positive LE indicates that the trajectories diffuse to initial conditions and corresponds to the chaotic system. Another scenario is a zero LE, which indicates a stable attractor of the orbits. In Figs. 1(e) and 2(e) LEs for the excitonic mode and the cavity mode with time evolutions are presented, respectively. As is shown, for the selection of appropriate parameters, the LEs evolve into positive values, which means the chaotic system for both the excitonic and cavity modes, that is, the dynamic evolution of the system is extremely sensitive to the minor changes of the initial conditions.

In the following numerical simulations, we investigate the influence of the controllable parameters  $f$ ,  $g$ ,  $\epsilon$ ,  $\xi$ , and  $\Delta$  on the chaotic dynamics under the time evolution from 0 to 40. Contour maps with different parameters are plotted under relatively stable chaotic dynamics from time 20 to 40.

To explore the influence of the parameter  $f$  that denotes the collective response of the many-exciton system to the cavity on the chaotic dynamics, we show the evolution of  $\text{Re}(\beta)(\alpha)$  and the LEs with different  $f$  in Fig. 3. We can see that initially the parameter  $f$  has very little impact on the chaotic dynamics of both the excitons and the cavity field. However, it has a significant influence on the chaotic dynamics for long times. A negative LE for the excitons [green solid line in Fig. 3(c)] corresponding to the periodic system dynamics for  $f = 0$  can change into chaotic dynamics [blue dotted line in Fig. 3(c)] for

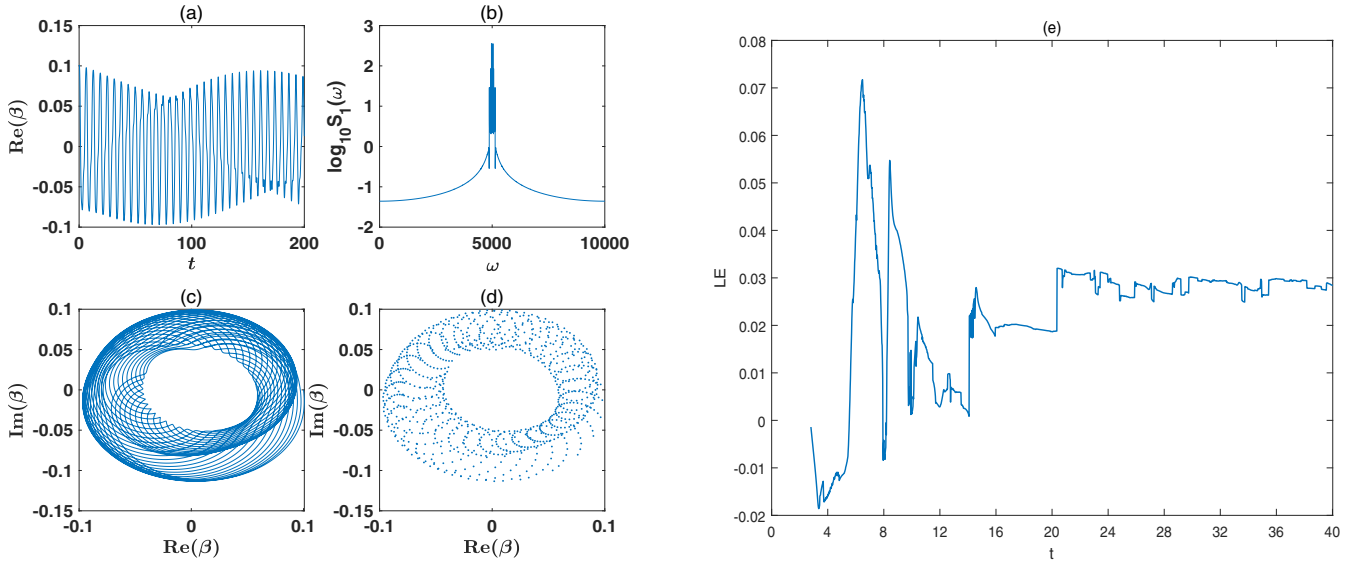


FIG. 1. Oscillation of the excitons plotted in (a) the temporal domain and (b) the frequency domain. Also plotted are (c) the stroboscopic phase space of the quantum trajectories and (d) Poincaré surface sections projected in the  $X_1[\text{Re}(\beta)]$ - $P_1[\text{Im}(\beta)]$  plane. (e) The LE for the excitons as time  $t$ . The initial conditions are  $\alpha = 0.1$  and  $\beta = 0.1$ . The parameters are  $\gamma_1 = \gamma_2 = 0.001$ ,  $g = 0.1$ ,  $\epsilon = 0.4$ ,  $f = 0.3$ ,  $\omega_{ph} = 2$ ,  $\omega_{ex} = 1$ ,  $\chi = 0.1$ , and  $\omega = 4$ . The unit of  $t$  is set equal to  $1/\omega_{ex}$ .

$f = 1$  with time from 14 to 22. Moreover, the intensity of the chaos of the cavity increases with  $f$  from 0 to 1 [see Fig. 3(d)]. Physically, the chaos of the system originally comes from the optoexcitonic nonlinearity, while the nonlinear strength will be enhanced with increasing  $f$ . It is worth noting at this moment that the  $f$  interaction results from the dipole-dipole-like nature of the exciton-exciton nonlinear interaction. We can also see in Figs. 3(e) and 3(f) that chaotic behavior persists even when  $f$  is approximately 0 with the long-time evolution. The main reason is that the chaos in this system arises as a result of not only  $f$ , but also the exciton nonlinearity terms  $\xi$  and the external laser term  $\epsilon$ .

In Fig. 4 we investigate the effect of the coupling constant  $g$  between the excitons and the cavity on the chaotic dynamics of the system. Taking the same parameters as before,  $g$  has a dramatic effect on the chaotic dynamics of the exciton and the cavity. The chaotic intensities of the excitons and the cavity field both increase with  $g$  from 0 to 0.2. We also note that intermittent chaos appears for excitons with the time evolution when  $g = 0$  [see the green solid line in Fig. 4(c)]. However, consistent chaos exists for the cavity with time when  $g = 0$  [see the green solid line in Fig. 4(d)] because the chaoticity in the cavity arises not only as the coupling term, but also as the pump field. It has been verified that the transmitted pump

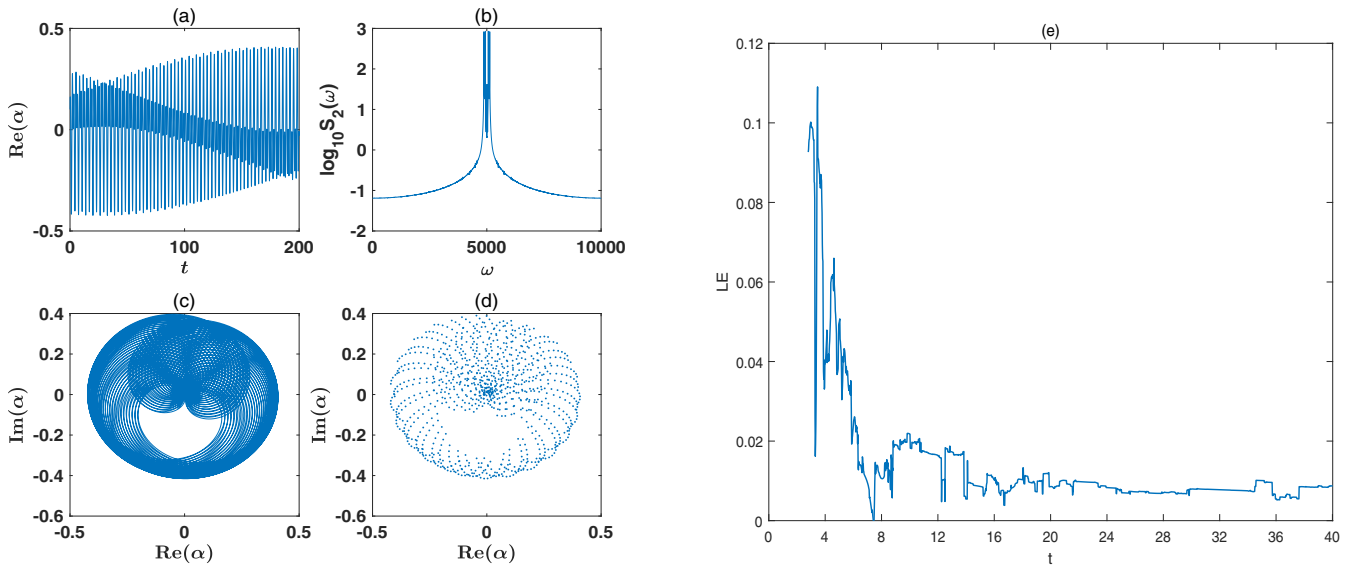


FIG. 2. Oscillation of the cavity plotted in (a) the temporal domain and (b) the frequency domain. Also plotted are (c) the stroboscopic phase space of the quantum trajectories and (d) Poincaré surface sections projected in the  $X_2[\text{Re}(\beta)]$ - $P_2[\text{Im}(\beta)]$  plane. (e) Largest Lyapunov exponent for the cavity field as time  $t$ . The initial conditions and choice of the parameters are the same as in Fig. 1.

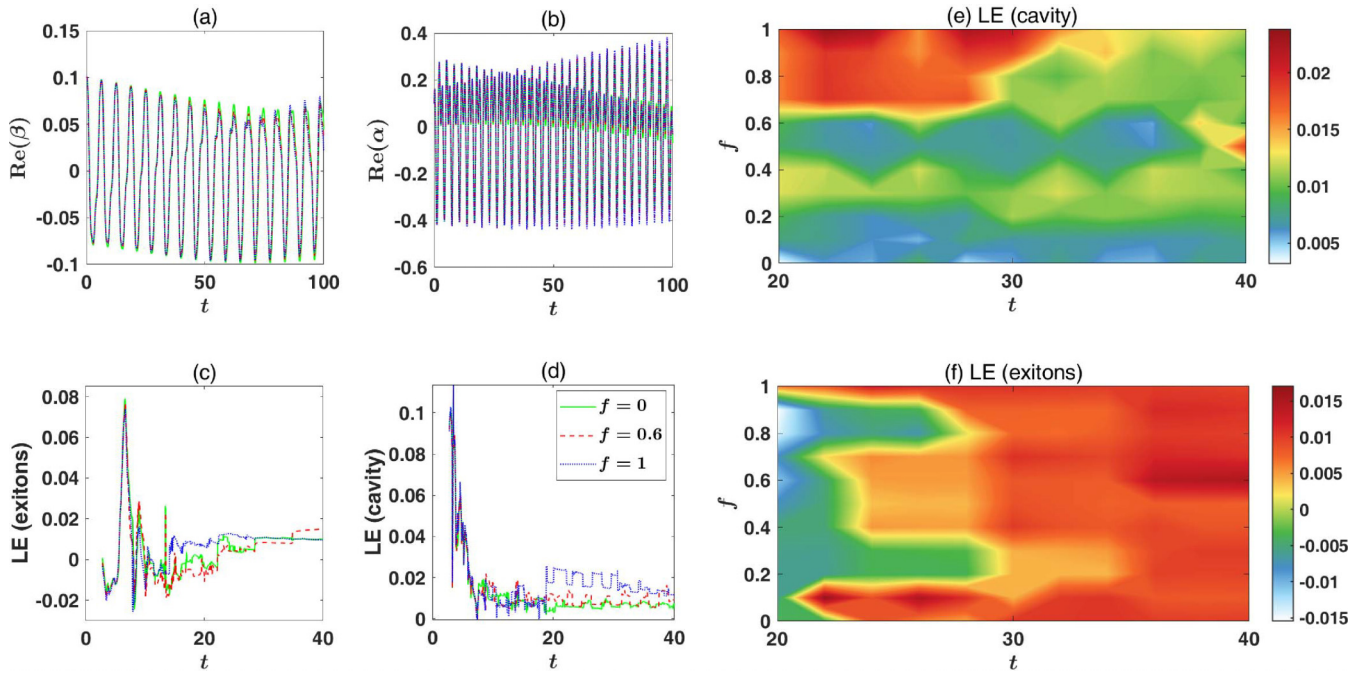


FIG. 3. Time evolution of the  $\text{Re}(\beta)(\alpha)$  and LEs of the excitons and the cavity with different  $f$ . The parameters are the same as in Fig. 1.

light is observed to transit from a fixed state to a region of periodic oscillations and finally to the chaotic regime through period-doubling bifurcation [7]. We also note that chaos for both the cavity and the excitons will disappear when  $g$  is too big (not shown here). While a larger  $g$  will lead to the linear term playing a major role, the nonlinear interaction that arises from the interaction between the excitons and the cavity is negligible compared to that of the light intensity and eliminates the chaotic dynamics.

In this system, another controllable parameter is  $\epsilon$ , which is related to the strength of the pump field. From Fig. 5 we can see that both the excitons and the cavity experience regular to chaotic behavior when the external laser increases from  $\epsilon = 0$  to 0.5. Moreover, independently chaotic motions will appear for both the excitons and the cavity with time evolution from about 5 to 7 even when  $\epsilon = 0$ . However, after the time reaches about 9, the chaos of the excitons and the cavity will fade away because of the energy dissipation, as shown in

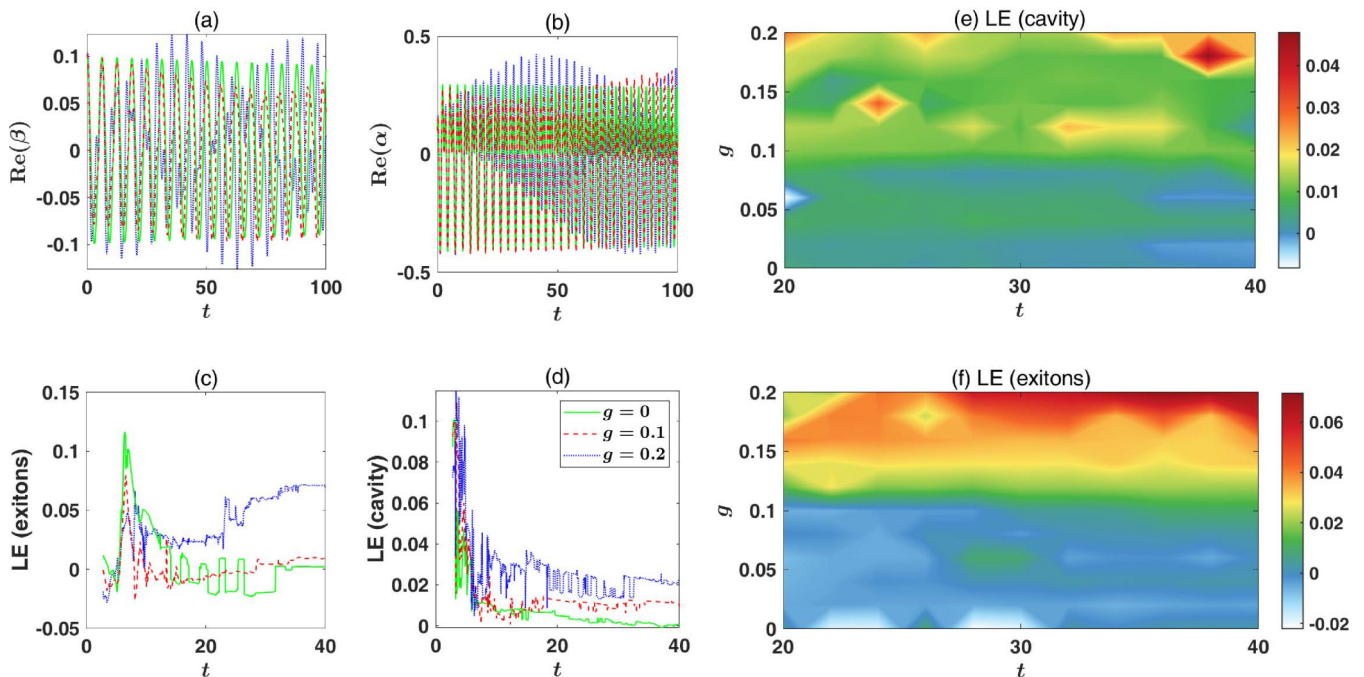


FIG. 4. Time evolution of the  $\text{Re}(\beta)(\alpha)$  and LEs of the excitons and the cavity with different  $f$ . The parameters are the same as in Fig. 1.

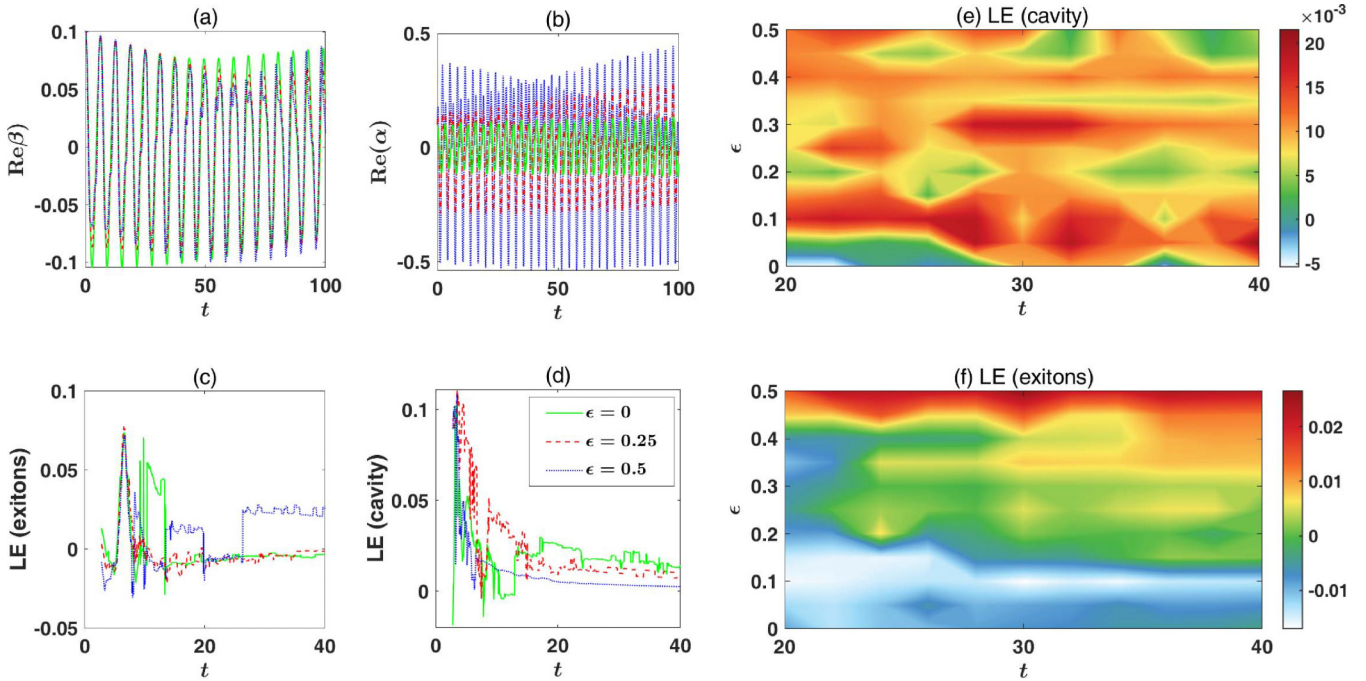


FIG. 5. Time evolution of the  $\text{Re}(\beta)(\alpha)$  and LEs of the excitons and the cavity with different  $\epsilon$ . The parameters are the same as in Fig. 1.

Fig. 5 (green solid lines). Fortunately, the chaos of both the exciton and the cavity can be recovered with the appearance of the external field. The values of the LE for the cavity are increased slightly but are greatly enhanced with the increase of the parameter  $\epsilon$ , as shown in Figs. 5(c) and 5(d). The results agree with previous studies [7]: With the help of the pump field, the transmitted pump light is observed to transit from a fixed state to a region of periodic oscillations and finally to the chaotic regime through period-doubling bifurcation [7]. The main cause of this phenomenon is that the nonlinear coupling strength between the excitonic mode and the cavity mode can be enhanced with the help of the pump field. Hence, the controllable parameter  $\epsilon$  allows us to control chaos generation in our system.

In Fig. 6 we investigate the influence of  $\xi$  on the chaotic dynamics of this system. It can be seen that the parameter  $\xi$ , which is related to the strength of the interaction between excitons, has a great influence on the chaotic dynamics of the excitons but little effect on the cavity mode. As shown in Figs. 6(c) and 6(d), the strength of the chaos for the cavity greatly increases but there is only a slightly change for the cavity with  $\xi$ . This phenomenon can be observed from the fourth term  $\xi \hat{b}^\dagger \hat{b}^\dagger \hat{b} \hat{b}$  in Eq. (1): The nonlinear effect between excitons increases with the enhancement of the parameter  $\xi$ . We also note that chaos still exists for both the exciton and the cavity when  $\xi = 0$ . According to the previous analysis, the generation of chaos is not only related to the parameter  $\xi$  but also depends on the strength of the interaction between excitons as well as the strength of the pump field.

To further explore the influence of the detuning  $\Delta = \omega_{ph} - \omega_{ex}$  on the chaotic dynamics, we present the evolution of the  $\text{Re}(\beta)(\alpha)$  and LEs in Fig. 7 with different detunings. We can see clearly that the excitons are nearly periodic for blue detuning when  $\Delta = 1$  [see Fig. 7(a)], which means no

chaos can be generated. However, chaos gradually appears with decreasing  $\Delta$ . This shows that small detuning induces a considerable exciton-cavity nonlinearity and increases the chaotic dynamics in both the excitonic mode and the cavity. We also find that the resonance case (detuning  $\Delta = 0$ ) can create optimal chaos in both the excitonic mode and the cavity mode. Physically, here the optical chaos mainly originates in the optoexcitonic nonlinearity, which is determined by the excitation of the excitons. The excitons are easily excited when the cavity and the excitons are resonant. Otherwise, the excitons cannot be excited and have no nonlinear effects. Notably, the appearance of regular or chaotic motion is very susceptible to the value of  $\Delta$ . By changing the optoexcitonic detuning, one can easily tune the semiconductor microcavity system in and out of chaos.

#### IV. DISCUSSION

Here we summarize the experimental implementation of our scenario. The microcavity sample can be excited using a Ti:Sa laser. The samples have been described in Refs. [46,57]. The quarter waveplate in front of the sample is used to excite with a circular polarization. A spatial filter is embodied in the near field of the reflected beam. Using the movable mirror mounted on a piezoelectric ceramic, the beam can be detected on a CCD camera, again in the near field. Thus we can study the spatial effects and choose the desirable position from which to observe. By means of a homodyne detection system, the frequency spectrum of the light emitted by the microcavity is detected. Thus, according to the result of the frequency spectrum, we can determine whether the cavity field is chaotic. However, the excitonic mode cannot be measured straightforwardly. To measure the quadratures of the exciton, we can use a method similar to that proposed by Giacobino *et al.* [55,58] and introduce another laser beam

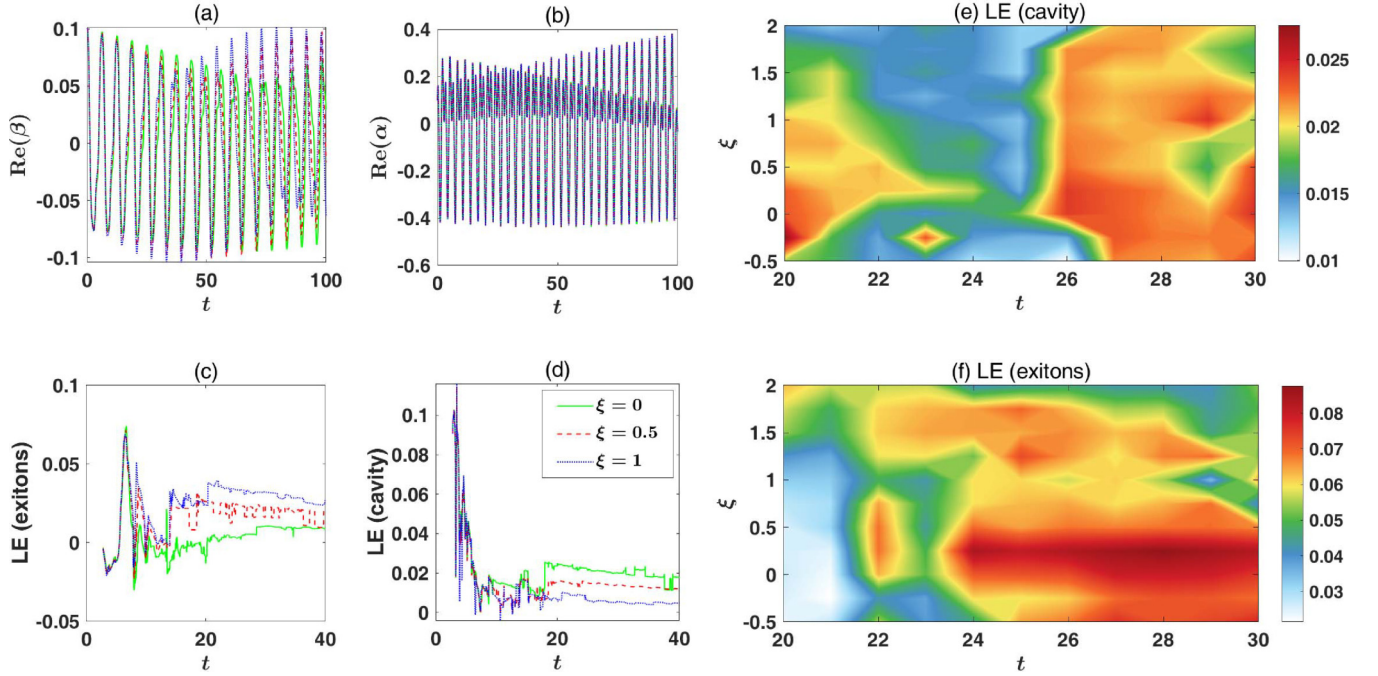


FIG. 6. Time evolution of the  $\text{Re}(\beta)$ ( $\alpha$ ) and LEs of the excitons and the cavity with different  $\xi$ . The parameters are the same as in Fig. 1.

which is mixed with the pump and signal beam on a beam splitter. The frequency spectrum of the photocurrents is analyzed with an rf spectrum analyzer. The reflected laser and the light scattered at the laser frequency yield a large peak at zero frequency which is filtered out. The signal given by the spectrum analyzer can be shown [58] to be proportional to the beat signal between the local oscillator and the light fluctuations emitted by the sample.

In our paper the system parameters are in units of  $\omega_{ex}$ . The related parameters in Eq. (1) are defined as  $g = -\omega_{ph}\sqrt{\frac{\epsilon_0\Delta_L}{2\omega_{ex}}}$ ,  $\xi = \frac{26\pi}{3V}R_y r_x^3$ , and  $f = -\frac{7\pi}{V}gr_x^3$ , where  $R_y$  is the exciton Rydberg with  $R_y = 1.0967758 \times 10^7 \text{ m}^{-1}$ ,  $\Delta_L$  is the exciton longitudinal-transverse splitting,  $r_x$  is the exciton Bohr radius, and  $V$  is the volume of a finite-size sample. For CdS, the experimental parameters are  $E_g = 2.586 \text{ eV}$ ,  $\omega_{ex} = 2.553 \text{ eV}$ ,

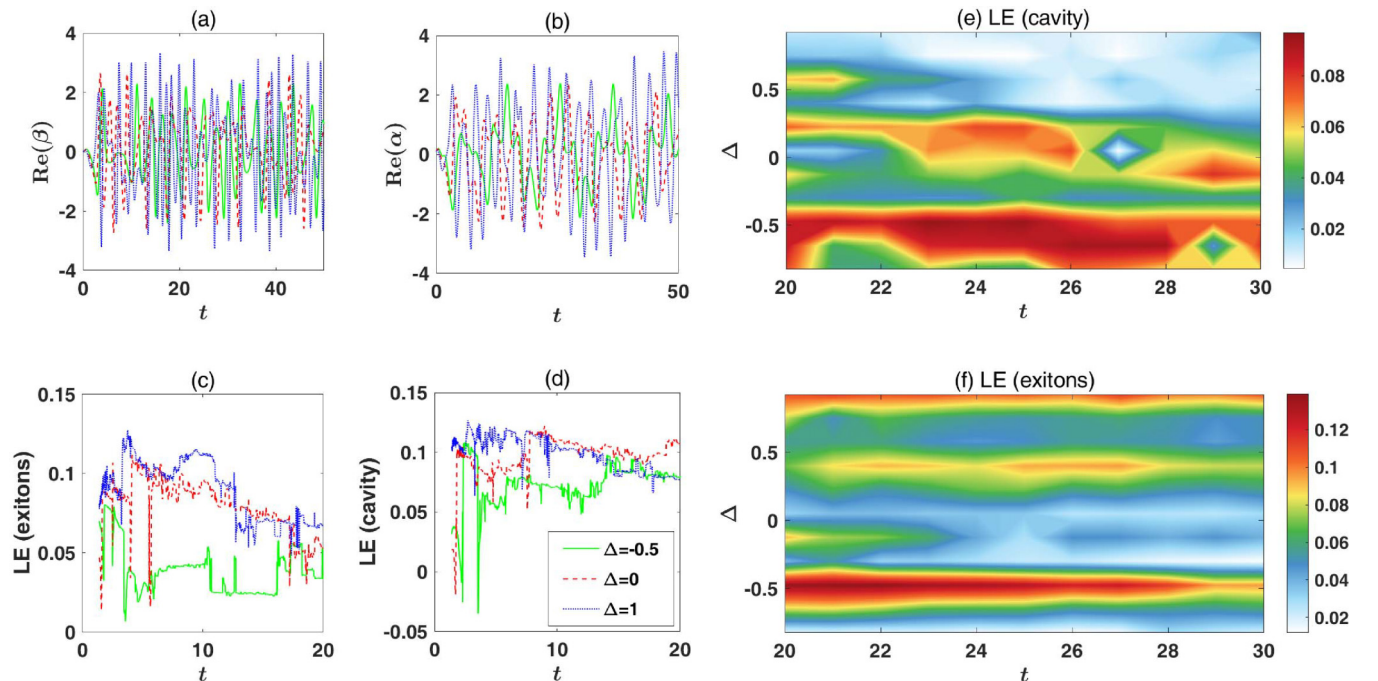


FIG. 7. Time evolution of the  $\text{Re}(\beta)$ ( $\alpha$ ) and LEs of the excitons and the cavity with different detuning  $\Delta = \omega_{ph} - \omega_{ex}$ . The parameters are the same as in Fig. 1.

$\Delta_L = 1$  meV,  $\epsilon_0 = 8$ , and  $r_x = 25.5\text{\AA}$ . According to these parameters, we can calculate the values  $g \approx -101$  meV,  $\xi V \approx 1.5 \times 10^{-17}$  meV cm<sup>3</sup>, and  $fV \approx 3.7 \times 10^{-17}$  meV cm<sup>3</sup> with  $V/v_{ex} = 4 \times 10^3$  ( $v_{ex} = 7 \times 10^{-20}$  cm<sup>3</sup> is the volume of an exciton). We can also use GaAs, whose parameters are  $E_g = 1.5$  eV,  $\omega_{ex} = 1.495$  eV,  $\Delta_L = 0.1$  meV,  $\epsilon_0 = 12$ , and  $r_x = 100$  Å, given the values  $g \approx -30$  meV,  $\xi V \approx 1.4 \times 10^{-16}$  meV cm<sup>3</sup>, and  $fV \approx 6.6 \times 10^{-16}$  meV cm<sup>3</sup> with  $V/v_{ex} = 4 \times 10^3$  [43,59]. In addition, the Rabi frequency of oscillation is  $\epsilon = 20\omega_m = 500$  GHz for a given energy level transition in a given light field. This denotes a form of electromagnetic radiation with frequencies ranging from 0.3 to 3000 GHz.

## V. CONCLUSION

We have studied a quantum well in a microcavity driven by an external classical field. Using a linearized fluctuation analysis, we investigated the chaotic dynamics of the excitonic mode and the cavity through numerical calculations. The related experimental parameters affecting the chaos of the system were examined. It has been shown that strong chaotic dynamics can be achieved by choosing the appropriate parameters. Moreover, chaos can be controlled for this scheme

by tuning the strength of the laser field  $\epsilon$ , nonlinear coefficients  $\xi$  and  $f$ , the coupling constant  $g$ , and the frequencies of the exciton  $\omega_{ex}$  and the cavity  $\omega_{ph}$ . The results of this research can be used to control the optical-excitonic chaotic dynamics in microcavity systems with a quantum well. Our study may contribute to the chaotic transfer of information and to improve the detection of otherwise undetectable signals in optical-excitonic systems.

It is worth mentioning that our calculations follow semiclassical motion. We expect this study about the chaotic behavior of a microcavity semiconductor containing a quantum well to be extended in the future. One may consider the quantum dynamics of the present system using the quantum state diffusion method [60,61].

## ACKNOWLEDGMENTS

This work was supported by NSFC through Grant No. 12265022, the Inner Mongolia Natural Science Foundation, China through Grant No. 2021MS01012, Natural Science Foundation of Fujian Province through Grant No. 2022J01548, and a project at Fuzhou University through Grant No. GXRC-21014.

- 
- [1] R. Laje and D. V. Buonomano, Robust timing and motor patterns by taming chaos in recurrent neural networks, *Nat. Neurosci.* **16**, 925 (2013).
- [2] F. Selmi, S. Coulibaly, Z. Lohmari, I. Sagnes, G. Beaudoin, M. G. Clerc, and S. Barbay, Spatiotemporal Chaos Induces Extreme Events in an Extended Microcavity Laser, *Phys. Rev. Lett.* **116**, 013901 (2016).
- [3] S. Coulibaly, M. G. Clerc, F. Selmi, and S. Barbay, Extreme events following bifurcation to spatiotemporal chaos in a spatially extended microcavity laser, *Phys. Rev. A* **95**, 023816 (2017).
- [4] V. M. Eskov, O. E. Filatova, V. V. Eskov, and T. V. Gavrilenko, The evolution of the idea of homeostasis: Determinism, stochasticity, and chaos-self-organization, *Biophysics* **62**, 809 (2017).
- [5] J. Wu, S.-W. Huang, Y. Huang, H. Zhao, J. Yang, J.-M. Liu, M. Yu, G. Lo, D.-L. Kwong, S. Duan, and C. W. Wong, Mesoscopic chaos mediated by Drude electron-hole plasma in silicon optomechanical oscillators, *Nat. Commun.* **8**, 15570 (2017).
- [6] J. Zhang, Y. X. Liu, W. M. Zhang, L. A. Wu, R. B. Wu, and T. J. Tarn, Deterministic chaos can act as a decoherence suppressor, *Phys. Rev. B* **84**, 214304 (2011).
- [7] F. Monifi, J. Zhang, Ş. K. Özdemir, B. Peng, Y.-x. Liu, F. Bo, F. Nori, and L. Yang, Optomechanically induced stochastic resonance and chaos transfer between optical fields, *Nat. Photon.* **10**, 399 (2016).
- [8] G. D. Vanwiggeren and R. Roy, Communication with chaotic lasers, *Science* **279**, 1198 (1998).
- [9] J. P. Goedgebuer, L. Larger, and H. Porte, Optical Cryptosystem Based on Synchronization of Hyperchaos Generated by a Delayed Feedback Tunable Laser Diode, *Phys. Rev. Lett.* **80**, 2249 (1998).
- [10] A. Argyris, D. Syvridis, L. Larger, V. Annovazzi-Lodi, P. Colet, I. Fischer, J. García-Ojalvo, C. R. Mirasso, L. Pesquera, and K. A. Shore, Chaos-based communications at high bit rates using commercial fibre-optic links, *Nature (London)* **438**, 343 (2005).
- [11] A. Uchida, K. Amano, M. Inoue, K. Hirano, S. Naito, H. Someya, I. Oowada, T. Kurashige, M. Shiki, S. Yoshimori, K. Yoshimura, and P. Davis, Fast physical random bit generation with chaotic semiconductor lasers, *Nat. Photon.* **2**, 728 (2008).
- [12] I. Reidler, Y. Aviad, M. Rosenbluh, and I. Kanter, Ultrahigh-Speed Random Number Generation Based on a Chaotic Semiconductor Laser, *Phys. Rev. Lett.* **103**, 024102 (2009).
- [13] K. Hirano, T. Yamazaki, S. Morikatsu, H. Okumura, H. Aida, A. Uchida, S. Yoshimori, K. Yoshimura, T. Harayama, and P. Davis, Fast random bit generation with bandwidth-enhanced chaos in semiconductor lasers, *Opt. Express* **18**, 5512 (2010).
- [14] T. J. Kippenberg, H. Rokhsari, T. Carmon, A. Scherer, and K. J. Vahala, Analysis of Radiation-Pressure Induced Mechanical Oscillation of an Optical Microcavity, *Phys. Rev. Lett.* **95**, 033901 (2005).
- [15] T. Carmon, H. Rokhsari, L. Yang, T. J. Kippenberg, and K. J. Vahala, Temporal Behavior of Radiation-Pressure-Induced Vibrations of an Optical Microcavity Phonon Mode, *Phys. Rev. Lett.* **94**, 223902 (2005).
- [16] F. Marquardt, J. G. E. Harris, and S. M. Girvin, Dynamical Multistability Induced by Radiation Pressure in High-Finesse Micromechanical Optical Cavities, *Phys. Rev. Lett.* **96**, 103901 (2006).
- [17] C. Metzger, M. Ludwig, C. Neuenhahn, A. Ortlieb, I. Favero, K. Karrai, and F. Marquardt, Self-Induced Oscillations in an Optomechanical System Driven by Bolometric Backaction, *Phys. Rev. Lett.* **101**, 133903 (2008).
- [18] S. Zaitsev, A. K. Pandey, O. Shtempluck, and E. Buks, Forced and self-excited oscillations of an optomechanical cavity, *Phys. Rev. E* **84**, 046605 (2011).

- [19] T. Carmon, M. C. Cross, and K. J. Vahala, Chaotic Quivering of Micron-Scaled On-Chip Resonators Excited by Centrifugal Optical Pressure, *Phys. Rev. Lett.* **98**, 167203 (2007).
- [20] D. Navarro-Urrios, N. E. Capuj, M. F. Colombano, P. D. García, M. Sledzinska, F. Alzina, A. Griol, A. Martínez, and C. M. Sotomayor-Torres, Nonlinear dynamics and chaos in an optomechanical beam, *Nat. Commun.* **8**, 14965 (2017).
- [21] D. W. Zhang, C. You, and X. Y. Lü, Intermittent chaos in cavity optomechanics, *Phys. Rev. A* **101**, 053851 (2020).
- [22] X. Y. Lü, H. Jing, J. Y. Ma, and Y. Wu,  $\mathcal{PT}$ -Symmetry-Breaking Chaos in Optomechanics, *Phys. Rev. Lett.* **114**, 253601 (2015).
- [23] *Microcavities and Photonic Bandgaps: Physics and Applications*, edited by J. G. Rarity and C. Weisbuch NATO Advanced Studies Institute, Series E: Applied Sciences, Vol. 324 (Kluwer, Dordrecht, 2012).
- [24] V. Savona, Z. Hradil, A. Quattropani, and P. Schwendimann, Quantum theory of quantum-well polaritons in semiconductor microcavities, *Phys. Rev. B* **49**, 8774 (1994).
- [25] S. Savasta and R. Girlanda, Quantum Optical Effects and Nonlinear Dynamics in Interacting Electron Systems, *Phys. Rev. Lett.* **77**, 4736 (1996).
- [26] X. D. Fan, M. C. Lonergan, Y. Z. Zhang, and H. L. Wang, Enhanced spontaneous emission from semiconductor nanocrystals embedded in whispering gallery optical microcavities, *Phys. Rev. B* **64**, 115310 (2001).
- [27] C. Weisbuch, M. Nishioka, A. Ishikawa, and Y. Arakawa, Observation of the Coupled Exciton-Photon Mode Splitting in a Semiconductor Quantum Microcavity, *Phys. Rev. Lett.* **69**, 3314 (1992).
- [28] H. Eleuch, Photon statistics of light in semiconductor microcavities, *J. Phys. B* **41**, 055502 (2008).
- [29] H. Ajiki and H. Ishihara, Entangled-photon generation in biexcitonic cavity QED, *J. Phys. Soc. Jpn.* **76**, 053401 (2007).
- [30] H. Oka and H. Ishihara, Effects of unbound two-exciton states on entangled photons generated from a cavity biexciton, *Phys. Stat. Sol. C* **5**, 2446 (2008).
- [31] C. Ciuti, P. Schwendimann, B. Deveaud, and A. Quattropani, Theory of the angle-resonant polariton amplifier, *Phys. Rev. B* **62**, R4825(R) (2000).
- [32] Y. X. Liu, C. C. Cao, and H. Cao, Effect of the exciton-exciton interaction on resonance fluorescence of excitons in a quantum well, *Phys. Rev. A* **61**, 023802 (2000).
- [33] J. Inoue, T. Brandes, and A. Shimizu, Renormalized bosonic interaction of excitons, *Phys. Rev. B* **61**, 2863 (2000).
- [34] Y.-X. Liu, C. P. Sun, S. X. Yu, and D. L. Zhou, Semiconductor-cavity QED in high- $Q$  regimes with  $q$ -deformed bosons, *Phys. Rev. A* **63**, 023802 (2001).
- [35] D. Erenso, R. Vyas, and S. Singh, Quantum well in a microcavity with injected squeezed vacuum, *Phys. Rev. A* **67**, 013818 (2003).
- [36] O. Bleu, J. Levinsen, and M. M. Parish, Interplay between polarization and quantum correlations of confined polaritons, *Phys. Rev. B* **104**, 035304 (2021).
- [37] E. A. Sete and H. Eleuch, Interaction of a quantum well with squeezed light: Quantum-statistical properties, *Phys. Rev. A* **82**, 043810 (2010).
- [38] A. Olaya-Castro, F. J. Rodríguez, L. Quiroga, and C. Tejedor, Restrictions on the Coherence of the Ultrafast Optical Emission from an Electron-Hole-Pair Condensate, *Phys. Rev. Lett.* **87**, 246403 (2001).
- [39] J. I. Perea and C. Tejedor, Polarization entanglement visibility of photon pairs emitted by a quantum dot embedded in a microcavity, *Phys. Rev. B* **72**, 035303 (2005).
- [40] P. R. Eastham and P. B. Littlewood, Finite-size fluctuations and photon statistics near the polariton condensation transition in a single-mode microcavity, *Phys. Rev. B* **73**, 085306 (2006).
- [41] C. Gies, J. Wiersig, M. Lorke, and F. Jahnke, Semiconductor model for quantum-dot-based microcavity lasers, *Phys. Rev. A* **75**, 013803 (2007).
- [42] A. Mukhopadhyay, B. Sen, K. Thapliyal, S. Mandal, and A. Pathak, Interaction of light and semiconductor can generate quantum states required for solid-state quantum computing: Entangled, steered and other nonclassical states, *Quantum Inf. Process.* **18**, 1 (2019).
- [43] B. A. Nguyen, Exciton-induced squeezed state of light in semiconductors, *Phys. Rev. B* **48**, 11732 (1993).
- [44] P. Schwendimann, C. Ciuti, and A. Quattropani, Statistics of polaritons in the nonlinear regime, *Phys. Rev. B* **68**, 165324 (2003).
- [45] H. Eleuch and R. Bennaceur, Nonlinear dissipation and the quantum noise of light in semiconductor microcavities, *J. Phys. B: At. Mol. Opt. Phys.* **6**, 189 (2004).
- [46] J. Ph. Karr, A. Baas, R. Houdré, and E. Giacobino, Squeezing in semiconductor microcavities in the strong-coupling regime, *Phys. Rev. A* **69**, 031802(R) (2004).
- [47] A. B. Mohamed and E. Hichem, Non-classical effects in cavity QED containing a nonlinear optical medium and a quantum well: Entanglement and non-Gaussianity, *Eur. Phys. J. D* **69**, 191 (2015).
- [48] Y. H. Ma, E. Wu, X. F. Zhang, Y. H. Dong, and X. G. Han, Entanglement generated in a semiconductor microcavity, *Int. J. Theor. Phys.* **50**, 3205 (2011).
- [49] W. Yan, T. Wang, X. M. Li, and Y. J. Jin, Electromagnetically induced transparency and theoretical slow light in semiconductor multiple quantum wells, *Appl. Phys. B* **108**, 515 (2012).
- [50] M. Wagner, H. Schneider, D. Stehr, S. Winnerl, A. M. Andrews, S. Scharfner, G. Strasser, and M. Helm, Observation of the Intraexciton Autler-Townes Effect in GaAs/AlGaAs Semiconductor Quantum Wells, *Phys. Rev. Lett.* **105**, 167401 (2010).
- [51] H. W. Wu, X. W. Mi, Y. G. Huang, and K. H. Song, Autler-Townes splitting and quantum confined Stark effect of sideband peak in asymmetric double quantum wells, *J. Appl. Phys.* **113**, 043105 (2013).
- [52] W. D. Rice, J. Kono, S. Zeybel *et al.*, Observation of Forbidden Exciton Transitions Mediated by Coulomb Interactions in Photoexcited Semiconductor Quantum Wells, *Phys. Rev. Lett.* **110**, 137404 (2013).
- [53] H. Eleuch and A. Prasad, Chaos and regularity in semiconductor microcavities, *Phys. Lett. A* **376**, 1970 (2012).
- [54] G. Messin, J. P. Karr, H. Eleuch, J. M. Courty, and E. Giacobino, Squeezed states and the quantum noise of light in semiconductor microcavities, *J. Phys.: Condens. Matter* **11**, 6069 (1999).
- [55] E. Giacobino, J. P. Karr, G. Messin, H. Eleuch, and A. Baas, Quantum optical effects in semiconductor microcavities, *C. R. Phys.* **3**, 41 (2002).



- [56] X. Y. Wang, L. G. Si, X. H. Lu, and Y. Wu, Static Casimir effect induced optical chaos in an optomechanical system, *J. Phys. B* **54**, 055402 (2021).
- [57] R. Houdré, C. Weisbuch, R. P. Stanley, U. Oesterle, and M. Illegems, Nonlinear Emission of Semiconductor Microcavities in the Strong Coupling Regime, *Phys. Rev. Lett.* **85**, 2793 (2000).
- [58] H. P. Yuen and V. W. S. Chan, Noise in homodyne and heterodyne detection, *Opt. Lett.* **8**, 177 (1983).
- [59] E. Hanamura, Theory of many Wannier excitons. I, *Phys. Soc. Jpn.* **37**, 1545 (1974).
- [60] N. Gisin and I. C. Percival, The quantum-state diffusion model applied to open systems, *J. Phys. A: Math. Gen.* **25**, 5677 (1992).
- [61] R. Schack and T. A. Brun, A C++ library using quantum trajectories to solve quantum master equations, *Comput. Phys. Commun.* **102**, 210 (1997).